Chapter 2

System of choice: Open interacting Bose gases

Simulations presented in this thesis mostly[1] concern themselves with simulations of interacting Bose gases in a lattice model with two-particle interactions[2]. Here those basic details of the model that are repeatedly referred to in the body of the thesis are introduced. Also, this choice of mesoscopic system from the wide variety whose simulations could have been attempted is motivated.

This chapter does not attempt to present a review of the state of knowledge on interacting Bose gases, as this is currently very extensive and doing so would unnecessarily lengthen the thesis without introducing any additional novelty. Instead, I recommend to the reader the excellent reviews on both theoretical and experimental aspects of Bose Einstein condensation in cold alkali gases by Leggett[30], Dalfovo *et al*[31], Parkins and Walls[32]. Topical also are the 1998 Nobel lectures of Chu[33], Cohen-Tannoudji[34], and Phillips[35] on laser cooling and magneto-optical trapping, as well as the reviews of evaporative cooling by Ketterle and van Druten[36] and Walraven[37]. An overview of recent developments can be found in e.g. the collection of articles in Nature *Insight on ultracold matter*[16, 17, 18, 19, 20]. Physical properties of interacting Bose gases pertinent to the analysis or interpretation of the

[1] Although not exclusively, see for example Chapter 6.

[2] In the most commonly used cold alkali-metal gas models these interactions are local as in a Bose-Hubbard model, and are then often referred to as "delta-function" interactions.

simulations in Parts B and C of this thesis are given in the relevant chapters.

2.1 Motivation

The choice to concentrate on cold dilute interacting Bose gas models when trying out the simulation methods developed in this thesis is motivated by the following considerations:

- The prime motivation is that mesoscopic systems that are very well described by these models are experimentally accessible. These are the cold dilute alkali-metal gases at temperatures below or near the Bose-Einstein condensation (BEC) temperature. In the last several years production of cold Bose gases of alkali-metal atoms has become almost routine, occurring in many tens of labs around the world. The largest interest (see Figure 2.1) has been in gases below the condensation temperature where quantum effects come to dominate the system even though it is mesoscopic or even approaching macroscopic in size. These were first realized in 1995 by Anderson *et al*[6] (^{87}Rb), Davis *et al*[7] (^{23}Na), and Bradley *et al*[8] (^{7}Li), by laser cooling the gas in a trap, and subsequently lowering the temperature even further by evaporative cooling. Three years later the first signatures of BEC were seen by Fried *et al*[9] in the somewhat different case of hydrogen. Presently, many variants of these systems are being investigated experimentally. For example, quasi-one-dimensional gases have been achieved[38, 39, 40], and coherent four-wave mixing between atom clouds has been observed[41], just to name a few of the experimental directions relevant to the models considered later in this thesis.

- A related argument is that there are phenomena in the experimental systems that are not precisely understood and appear quite resistant to conclusive theoretical analysis by approximate methods. This invites a first-principles investigation.

  Most of these occur in situations where there is a transition or interplay between disordered high temperature behavior well above condensation temper-

ature T_c, and the pure many-body quantum states approached as $T \to 0$. The first can be treated with kinetic theories, while the latter is very well described by the Gross-Pitaevskii (GP)[42, 43, 44] mean-field equations, or Bogoliubov theory[45][3]. As usual in physical systems, the intermediate regime is the most complicated and is the place where first-principles simulations are the most needed.

Examples of such issues where first-principles simulations can make a step forward to full understanding are, for example:

1. The behavior of the system during initial condensation, when the $T \approx T_c$ barrier is crossed. This includes issues such as "does the always condensate form in the ground state, or is (at least metastable) condensation into excited states possible?" There are some indications that condensates may occur e.g. in states of non-zero centre-of-mass motion[15].
2. Is the exact ground state of a BEC the same as that obtained by semi-classical GP methods?
3. Dynamics of condensates during atom interferometry.
4. The decoupling of atoms from the trapped condensate in an atom laser arrangement. How is the emitting condensate disturbed, and in what state are the pulses emitted?
5. Scattering of atoms into empty momentum modes when condensates collide[41].
6. Heating and other processes that eventually destroy the condensate in experiments.

It is worth noting that most of the above processes usually involve coupling of the condensate to an external environment. This is further indication that a simulation method capable of handling open systems is desirable.

- Not only is the field of Bose-Einstein condensation experimentally accessible, but the sheer amount of research on the topic has been growing (and continues

[3]At finite temperatures , but significantly below T_c

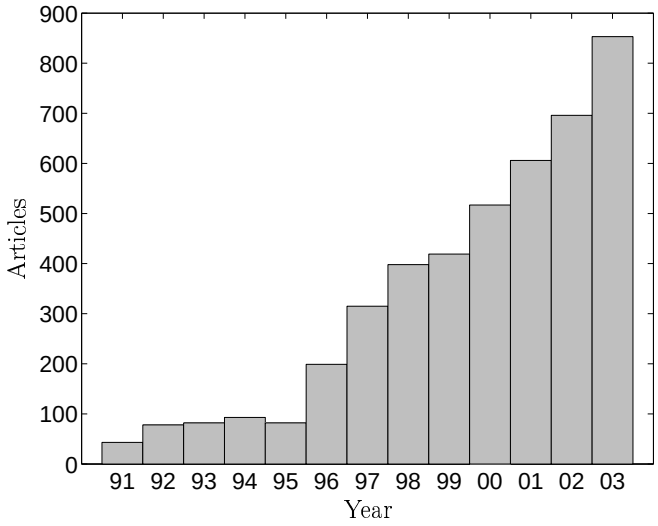

Figure 2.1: **Papers published in refereed journals** (by year) on the topic of Bose-Einstein condensation. Based on a search for the keywords "Bose Einstein condens*" or "Bose condens*" through titles and abstracts in the ISI "Web of Science" citation database (http://wos.isiglobalnet.com/) on 11 Feb 2004. Note the rapid increase after the first successful BEC experiments in 1995.

to grow) at a great rate (see Figure 2.1). This would indicate that some of the predictions made may be verified rapidly.

- Lastly, but importantly, many-mode simulations of similar systems have been successful with a phase-space method (the positive P distribution[10, 11]). Some examples of this include simulations of evaporative cooling of a Bose gas to the beginning of condensation[14, 15, 46], as well as simulations of optical soliton propagation in nonlinear Kerr media[12, 13], which have a similar form of nonlinearity to (2.17) — quadratic in local particle density. The gauge distributions developed in this thesis include the positive P distribution as a special case, and improve on it. This previous success is an indication that the newer methods are likely to lead to significant results with these systems.

2.2 Field model with binary interactions

Consider a $\mathcal{D}$-dimensional boson field $\widehat{\Psi}(\mathbf{x})$ undergoing two-particle interactions. After second quantization the Hamiltonian of the system can be written as

$$\begin{aligned}\widehat{H} &= \int d^{\mathcal{D}}\mathbf{x}\left\{\frac{\hbar^2}{2m}\frac{\partial\widehat{\Psi}^\dagger(\mathbf{x})}{\partial\mathbf{x}}\frac{\partial\widehat{\Psi}(\mathbf{x})}{\partial\mathbf{x}} + V^{\text{ext}}(\mathbf{x})\widehat{\Psi}^\dagger(\mathbf{x})\widehat{\Psi}(\mathbf{x})\right\} \\ &+ \frac{1}{2}\int d^{\mathcal{D}}\mathbf{x}d^{\mathcal{D}}\mathbf{y}U(\mathbf{x}-\mathbf{y})\widehat{\Psi}^\dagger(\mathbf{x})\widehat{\Psi}^\dagger(\mathbf{y})\widehat{\Psi}(\mathbf{x})\widehat{\Psi}(\mathbf{y}). \qquad (2.1)\end{aligned}$$

The bosons have mass m, move in $\mathcal{D}$-dimensional space whose coordinates are $\mathbf{x}$, experience an external conservative potential $V_{\text{ext}}(\mathbf{x})$, and an interparticle potential $U(\mathbf{r}) = U(-\mathbf{r})$ where $\mathbf{r}$ is the spacing between two particles. The field operators $\widehat{\Psi}^\dagger(\mathbf{x})$ and $\widehat{\Psi}(\mathbf{x})$ are creation and destruction operators on bosons at $\mathbf{x}$, and obey the usual commutation relations

$$\left[\widehat{\Psi}(\mathbf{x}), \widehat{\Psi}^\dagger(\mathbf{y})\right] = \delta^{\mathcal{D}}(\mathbf{x}-\mathbf{y}). \qquad (2.2)$$

The total number of bosons is

$$\widehat{N} = \int d^{\mathcal{D}}\mathbf{x}\widehat{\Psi}^\dagger(\mathbf{x})\widehat{\Psi}(\mathbf{x}). \qquad (2.3)$$

In a typical Bose-Einstein condensation experiment with cold trapped alkali-metal gases the trapping potential V_{ext} is parabolic, in general non-spherical.

Three-body[4] processes are not included in the model. While these can be neglected for most contemporary experiments with cold rarefied alkali-metal gases or BECs, they can become significant when density is high enough, or when one operates near a Feshbach resonanace, requiring modifications to the model. (For example, three-body recombination into molecules[47, 48] can play an important role in loss of atoms from a BEC).

2.3 Reduction to a lattice model

To allow computer simulations, (2.1) must be reduced to a lattice form. Provided the lattice is sufficiently fine to resolve all features, no change in physical interpretation occurs.

[4]Strictly speaking, all $N > 2$ body.

One issue to keep in mind, however, is that some care must be taken when going from a continuum to a lattice model to make sure that the behavior of the latter at length scales longer than the lattice spacing is the same — i.e. that the lattice model has been renormalized.

One way to do this is to impose:

1. A spatial box size in each dimension L_d,

2. A momentum cutoff in Fourier space $k_d^{\max}$,

where spatial dimensions have been labeled by $d = 1, \ldots, \mathcal{D}$. In this case one proceeds by expressing all spatially-varying functions (generically called $f(\mathbf{x})$) in Fourier modes as

$$f(\mathbf{x}) = \left(\prod_d \frac{\sqrt{2\pi}}{L_d} \right) \sum_{\widetilde{\mathbf{n}}} \widetilde{f}_{\widetilde{\mathbf{n}}} e^{i \mathbf{k}_{\widetilde{\mathbf{n}}} \cdot \mathbf{x}}, \tag{2.4}$$

where the index $\widetilde{\mathbf{n}} = \{\widetilde{n}_1, \ldots, \widetilde{n}_{\mathcal{D}}\}$ has an integer component $\widetilde{n}_d = 0, \pm 1, \pm 2, \ldots$ for each dimension. The wave vector $\mathbf{k}_{\widetilde{\mathbf{n}}} = \{k_1(\widetilde{n}_1), \ldots, k_{\mathcal{D}}(\widetilde{n}_{\mathcal{D}})\}$ also contains $\mathcal{D}$ components

$$k_d(\widetilde{n}_d) = 2\pi \widetilde{n}_d / L_d. \tag{2.5}$$

This has imposed the spatial box size, and now we also impose a momentum cutoff $k_d^{\max}$ by truncating all terms in (2.4) for which any $|k_d(\widetilde{n}_d)| > k_d^{\max}$. That is,

$$f(\mathbf{x}) \to f_{\text{cut}}(\mathbf{x}) = \left(\prod_d \frac{\sqrt{2\pi}}{L_d} \right) \sum_{|\widetilde{n}_1| \le L_1 k_1^{\max}/2\pi} \cdots \sum_{|\widetilde{n}_{\mathcal{D}}| \le L_{\mathcal{D}} k_{\mathcal{D}}^{\max}/2\pi} \widetilde{f}_{\widetilde{\mathbf{n}}} e^{i \mathbf{k}_{\widetilde{\mathbf{n}}} \cdot \mathbf{x}}. \tag{2.6}$$

This leaves an M_d point lattice in each dimension, with $M_d = 1 + 2\,\text{int}\,[L_d k_d^{\max}/2\pi]$, when int$[\,\cdot\,]$ gives the integer value (rounded down).

The lattice points in Fourier space k_d have been defined by (2.5), the function values there are $\widetilde{f}_{\widetilde{\mathbf{n}}}$, while the function values in normal space $f_{\mathbf{n}}$ are given by the discrete inverse Fourier transform of the $\widetilde{f}_{\widetilde{\mathbf{n}}}$:

$$f_{\mathbf{n}} = f_{\text{cut}}(\mathbf{x}_{\mathbf{n}}). \tag{2.7}$$

Here the spatial lattice is $\mathbf{x}_{\mathbf{n}} = \{x_1(n_1), \ldots, x_{\mathcal{D}}(n_{\mathcal{D}})\}$ given by

$$x_d(n_d) = n_d \Delta x_d, \tag{2.8}$$

with spacing $\Delta x_d = L_d/M_d$. The index $\mathbf{n}$ is composed of non-negative integers $\mathbf{n} = \{n_1, \ldots, n_{\mathcal{D}}\} : n_d = 0, 1, \ldots, M_d - 1$.

The lattice model is physically equivalent to the continuum field model provided that

1. No features occur on length scales $\approx L_d$ or greater.

2. The truncated Fourier components ($\widetilde{f}_{\tilde{\mathbf{n}}}$ corresponding to any $k_d > k_d^{\max}$) are negligible so that for all practical purposes $f(\mathbf{x}) = f_{\rm cut}(\mathbf{x})$. In other words, no features occur on length scales $\approx \Delta x_d$ or smaller.

Conversely, in cases when some processes occur entirely on length scales smaller than the lattice spacings Δx_d, the lattice model may be renormalized in non-trivial ways (so that $f_{\mathbf{n}} \neq f(\mathbf{x_n})$) to still be physically equivalent to the continuum model on lattice spacing length scales. An example is outlined in Section 2.4.

Proceeding in this manner for the case of extended interparticle interactions (2.1), and using the lattice notation of (2.4), (2.6), and (2.7), let us define the lattice annihilation operators

$$\hat{a}_{\mathbf{n}} = \widehat{\Psi}_{\mathbf{n}} \sqrt{\prod_d \Delta x_d}, \tag{2.9}$$

which obey the boson commutation relations

$$\left[\widehat{a}_{\mathbf{n}}, \widehat{a}^\dagger_{\mathbf{m}}\right] = \delta_{\mathbf{nm}}. \tag{2.10}$$

The particle number operator at lattice point $\mathbf{n}$ is

$$\widehat{n}_{\mathbf{n}} = \widehat{a}^\dagger_{\mathbf{n}} \widehat{a}_{\mathbf{n}}. \tag{2.11}$$

With these, one obtains the expression:

$$\widehat{H} \to \sum_{\mathbf{nm}} \left[\hbar\omega_{\mathbf{nm}} \widehat{a}^\dagger_{\mathbf{n}} \widehat{a}_{\mathbf{m}} + \frac{1}{2} u_{\mathbf{nm}} \widehat{n}_{\mathbf{n}} \left(\widehat{n}_{\mathbf{m}} - \delta_{\mathbf{nm}}\right) \right]. \tag{2.12}$$

In this normally ordered expression, the frequencies $\omega_{\mathbf{nm}} = \omega^*_{\mathbf{mn}}$ come from the kinetic energy and external potential. They produce a local particle number dependent energy, and linear coupling to other sites, the latter arising only from kinetic

processes. The frequencies $\omega_{\mathbf{nm}}$ are explicitly

$$\omega_{\mathbf{nm}} = \omega^*_{\mathbf{mn}} = \frac{\delta_{\mathbf{nm}}}{\hbar} V^{\mathrm{ext}}_{\mathbf{n}} + \frac{\hbar}{2m} \left(\prod_d \frac{\Delta x_d}{\sqrt{2\pi}} \right) K^{(2)}_{\mathbf{n}-\mathbf{m}}, \tag{2.13}$$

where the function $K^{(2)}$ is the $\mathcal{D}$-dimensional discrete inverse Fourier transform of $|\mathbf{k}|^2 = \sum_d k_d^2$. That is,

$$K^{(2)}_{\mathbf{n}} = \left(\prod_d \frac{\sqrt{2\pi}}{L_d} \right) \sum_{\widetilde{\mathbf{n}}} |\mathbf{k}_{\widetilde{\mathbf{n}}}|^2 e^{i\mathbf{k}_{\widetilde{\mathbf{n}}} \cdot \mathbf{x}_{\mathbf{n}}}. \tag{2.14}$$

The interparticle potential can also be discretized on the lattice, however there are a few subtleties caused by the finite box lengths L_d. Let us define the lattice mutual interaction strength $U_{\mathbf{n}} = U_{\mathrm{cut}}(\mathbf{x}_{\mathbf{n}})$ in the notation of (2.7) and (2.6). At first glance, the lattice scattering terms might be $u_{\mathbf{nm}} = U_{\mathbf{n}-\mathbf{m}}$ since $x_d(n_d) \propto n_d$, but there are two issues that complicate matters:

1. One has only non-negative lattice labels $\mathbf{n}$ and coordinates $x_d(n_d)$, as seen from (2.8).

2. The Fourier decomposition on a box of side lengths L_d implicitly assumes periodic boundary conditions, so e.g. particles at lattice points $\mathbf{n} = 0$ and $\mathbf{m} = \{M_1 - 1, \ldots, M_{\mathcal{D}} - 1\}$ are effectively in very close proximity.

In the continuum field model the interparticle potential is symmetric ($U(\mathbf{r}) = U(-\mathbf{r})$), so to impose periodicity on length scales L_d, the lattice interparticle potential should obey $U_{\mathbf{n}} = U_{\{M_1 - n_1, n_2, \ldots, n_{\mathcal{D}}\}} = \cdots = U_{\{n_1, n_2, \ldots, M_{\mathcal{D}} - n_{\mathcal{D}}\}}$. This symmetry then lets us write the scattering terms as

$$u_{\mathbf{nm}} = u_{\mathbf{mn}} = U_{|\mathbf{n}-\mathbf{m}|}, \tag{2.15}$$

where the notation means $|\mathbf{n} - \mathbf{m}| = \{|n_1 - m_1|, \ldots, |n_{\mathcal{D}} - m_{\mathcal{D}}|\}$. For the lattice model to be equivalent to an open continuum field model also requires $U_{\mathbf{n}}$ to be negligible when any $n_d \approx \mathcal{O}(M_d/2)$.

2.4 Locally interacting lattice model

The majority of mesoscopic experiments with interacting Bose gases where quantum mechanical features have been seen use alkali-metal atoms (Li, Na, K, Rb, Cs,

and also H) in or near the BEC regime (see also Section 2.1), where a significant simplification of the lattice Hamiltonian (2.12) can be made.

Broadly speaking, what is required is that only binary collisions be relevant, and that these occur on length scales much smaller than all other relevant length scales of the system, *including the lattice spacings* Δx_d. The simple-minded continuum to lattice procedure of the previous Section 2.3 no longer suffices, because the interparticle interactions occur at momenta well above $k_d^{\max}$. Detailed consideration to this renormalization is given in Section IV of the aforementioned review by Leggett[30], and in even more detail by Dalibard[49] and Wiener *et al*[50]. The reasoning for single-species cold alkali-metal Bose gases is (in brief) as follows:

- The leading term in inter-atomic potentials at long range $\gtrsim 5$Å for the alkali-metal atoms is the van der Waals interaction $\propto 1/|\mathbf{r}|^6$.

- This potential gives a van der Waals length $r_{\rm vdw}$ and energy $E_{\rm vdw} \sim \hbar^2/mr_{\rm vdw}^2$ characteristic of the atom species, which are the typical extent and binding energy of the largest bound state. For the alkali-metals $E_{\rm vdw}$ is of order $0.1 - 1$mK, except for hydrogen, which has $E_{\rm vdw} \approx 3$K.

- The binding energy of these states is much higher than thermal energies at or near the BEC condensation temperature for these atoms (typically, $T_c \approx \mathcal{O}\,(100\text{nK})$). For atom pairs with relative orbital angular momentum $l_{\rm rel} \neq 0$, the scattering strength is smaller than s-wave scattering ($l_{\rm rel} = 0$) by a factor of $(k_BT/E_{\rm vdw})^{l_{\rm rel}}$[30]. Conclusion: for $k_BT \ll E_{\rm vdw}$ only s-wave scattering interactions need be considered.

- For van der Waals potentials, s-wave scattering at low energies can be characterized by a single parameter, the s-wave scattering length a_s (see e.g. Landau and Lifshitz[51], Sec. 108). This is typically of similar size to $r_{\rm vdw}$. (e.g. for ^{87}Rb, $a_s = 5.77$nm [52]), and can be considered to be roughly the radius scale of an "equivalent" hard sphere (For indistinguishable bosons, the scattering cross-section is $8\pi a_s^2$).

- If the s-wave scattering length is *much smaller than all other relevant length*

scales of the system, then the exact inter-atom interaction can be replaced by a local lattice interaction where $u_{\mathbf{nm}} \propto \delta_{\mathbf{nm}}$ in the formalism of (2.12). Relevant length scales include the de Broglie wavelength of the fastest atoms, the interparticle spacing, the trap size, the transverse thickness (in the case of 2D or 1D systems), and *the lattice spacing* Δx_d.

Following this broad line of argument, it can be shown[49, 50, 30] that for two indistinguishable bosons in 3D, the scale-independent coupling constant g is given by

$$g = \frac{4\pi\hbar^2 a_s}{m}. \tag{2.16}$$

This then leads to a lattice Hamiltonian of the form

$$\widehat{H} = \sum_{\mathbf{nm}} \hbar\omega_{\mathbf{nm}} \widehat{a}^\dagger_{\mathbf{n}} \widehat{a}_{\mathbf{m}} + \hbar\chi \sum_{\mathbf{n}} \widehat{n}_{\mathbf{n}}(\widehat{n}_{\mathbf{n}} - 1), \tag{2.17}$$

with the (scale-dependent) lattice self-interaction strength being

$$\chi = \frac{g}{2\hbar \prod_d \Delta x_d}. \tag{2.18}$$

In the case of an effectively one- or two-dimensional gas of indistinguishable bosons, the coupling constant is instead given by

$$g = \frac{4\pi\hbar^2 a_s}{\lambda_0 m} \tag{2.19}$$

where λ_0 is, respectively, the effective thickness or cross-section in the transverse (collapsed) dimensions.

2.5 Open dynamic equations of motion

For a wide range of physical situations the interaction of an open system with its environment can be considered Markovian, and in this situation can be modeled with a master equation, where the evolution of the density matrix is dependent only on its present value, with no time lag effects. Broadly speaking, this means that any information about the system received by the environment via interactions is

dissipated much faster than the system dynamics we perceive. Hence, no feedback into the system occurs.

Under these conditions the equation of motion for the density matrix of the system can be written (in Linblad form) as:

$$\frac{\partial\widehat{\rho}}{\partial t} = \frac{1}{i\hbar}\left[\widehat{H},\widehat{\rho}\right] - \frac{1}{2}\sum_j\left[\widehat{L}_j^\dagger\widehat{L}_j\widehat{\rho} + \widehat{\rho}\widehat{L}_j^\dagger\widehat{L}_j\right] + \sum_j \widehat{L}_j\widehat{\rho}\widehat{L}_j^\dagger. \tag{2.20}$$

The Linblad operators $\widehat{L}_j$ represent various coupling processes to the environment, and their number depends on the details of the system-environment interactions. Note that $\widehat{\rho}$ is the reduced interaction picture density matrix of the (Bose gas + environment) system, traced over the environment. Some examples of common processes are:

Single-particle losses to a standard[5] zero temperature heat bath with rates $\gamma_{\mathbf{n}}$ at $\mathbf{x_n}$:

$$\widehat{L}_{\mathbf{n}} = \widehat{a}_{\mathbf{n}}\sqrt{\gamma_{\mathbf{n}}}. \tag{2.21}$$

Exchange with a finite temperature heat bath with coupling strength proportional to $\gamma_{\mathbf{n}}$ at $\mathbf{x_n}$:

$$\begin{aligned}\widehat{L}_{\mathbf{n}} &= \widehat{a}_{\mathbf{n}}\sqrt{\gamma_{\mathbf{n}}(1+\overline{n}_{\rm bath})},\\ \widehat{L}'_{\mathbf{n}} &= \widehat{a}^\dagger_{\mathbf{n}}\sqrt{\gamma_{\mathbf{n}}\overline{n}_{\rm bath}},\end{aligned} \tag{2.22}$$

Where the sum in (2.20) is taken over both terms in $\widehat{L}_{\mathbf{n}}$ and $\widehat{L}'_{\mathbf{n}}$. For the standard heat bath with energy $\hbar\omega_{\rm bath}$ per particle for all modes, $\overline{n}_{\rm bath}$, the mean number of particles per mode, is given by the Bose-Einstein distribution expression

$$\overline{n}_{\rm bath} = 1/[\exp(\hbar\omega_{\rm bath}/k_BT) - 1], \tag{2.23}$$

and hence for a zero temperature bath $\overline{n}_{\rm bath} = 0$.

Two-particle (at a time) losses to the standard zero temperature heat bath[11] with rate $\gamma^{(2)}_{\mathbf{n}}$ at $\mathbf{x_n}$:

$$\widehat{L}_{\mathbf{n}} = \widehat{a}^2_{\mathbf{n}}\sqrt{\gamma^{(2)}_{\mathbf{n}}}. \tag{2.24}$$

[5]The Hamiltonian of the heat bath is taken to be $\widehat{H} = \hbar\omega_{\rm bath}\sum_j\left(\widehat{b}_j^\dagger\widehat{b}_j + \frac{1}{2}\right)$ with $\widehat{b}_j$ being the annihilation operator for the jth heat bath subsystem.

Coherent gain from a driving field $\varepsilon_{\mathbf{n}}$ at $\mathbf{x}_{\mathbf{n}}$ can be modeled by adding a term of the form

$$\widehat{H}_c \;=\; i\hbar \sum_{\mathbf{n}} \left[\varepsilon_{\mathbf{n}} \widehat{a}^{\dagger}_{\mathbf{n}} - \varepsilon^{*}_{\mathbf{n}} \widehat{a}_{\mathbf{n}}\right] \tag{2.25}$$

to the Hamiltonian.

Details of the derivation of the loss/gain expressions (like those above, or more general) can be found e.g. in Gardiner[53], Chapter 10, or Louisell[54, 55].

2.6 Thermodynamic equations of motion

The (un-normalized) density matrix of a grand canonical ensemble in contact with a bath at temperature T and with chemical potential μ is given by

$$\widehat{\rho}_u = \exp\left[-(\widehat{H} - \mu\widehat{N})/k_B T\right] = e^{-\widehat{K}\tau}. \tag{2.26}$$

In the second expression the "imaginary time"[6] $\tau = 1/k_B T$ and the "Kamiltonian" $\widehat{K}$ have been introduced.

The rate of change of $\widehat{\rho}_u$ with τ can be written as[7]

$$\frac{\partial \widehat{\rho}_u}{\partial \tau} = -\frac{1}{2}\left[\frac{\partial \widehat{K}\tau}{\partial \tau}, \widehat{\rho}_u\right]_{+} = -\frac{\partial \widehat{K}\tau}{\partial \tau}\widehat{\rho}_u, \tag{2.27}$$

provided that

$$\left[\frac{\partial \widehat{K}}{\partial \tau}, \widehat{K}\right] = 0. \tag{2.28}$$

For the Hamiltonian here ((2.12) or (2.17)), the equation of motion can be written

$$\frac{\partial \widehat{\rho}_u}{\partial \tau} = \left[\mu_e(\tau)\widehat{N} - \widehat{H}\right]\widehat{\rho}_u, \tag{2.29}$$

where the "effective" chemical potential is

$$\mu_e(\tau) = \frac{\partial[\tau\mu(\tau)]}{\partial \tau}. \tag{2.30}$$

[6] So called because of the similarity of the left equality of (2.27) to (2.20) with t replaced by $i\hbar\tau/2$, and $\widehat{L}_j = 0$.

[7] $[\widehat{A}, \widehat{B}]_{+} = \widehat{A}\widehat{B} + \widehat{B}\widehat{A}$.

The condition (2.28) implies, in this case, that only the chemical potential $\mu(T)$ can be temperature dependent[8]

The utility of this equation stems from the fact that the grand canonical ensemble at $\tau = 0$ (i.e. high temperature $T \to \infty$) is known, and given by the simple expression

$$\widehat{\rho}_u(0) = \exp\left[-\lambda_n \widehat{N}\right], \tag{2.31}$$

where

$$\lambda_n = -\lim_{\tau \to 0} \left[\tau \mu(\tau)\right], \tag{2.32}$$

and the initial mean number of particles per lattice site is

$$\overline{n}_0 = \left[e^{\lambda_n} - 1\right]^{-1}. \tag{2.33}$$

This leads to initial conditions for the stochastic simulation that can be efficiently sampled in most cases. Finite temperature results are then obtained by evolving the system forward in τ.

[8]Strictly speaking, a constant (in space) external potential V^{ext} may also be temperature dependent, but this is physically equivalent to a correction to μ. Quantities such as g and $V^{\text{ext}}(\mathbf{x})$ must be constant with T for (2.29) to hold.